Molecular Simulation
Vol. 35, Nos. 1–2, January–February 2009, 70–78

Taylor & Francis
Taylor & Francis Group

Molecular simulations of hydrogen and methane permeation through pore mouth modified zeolite membranes

Sang Eun Jee[a], Alan J.H. McGaughey[b] and David S. Sholl[a]*

[a]*School of Chemical and Biomolecular Engineering, Georgia Institute of Technology, 311 Ferst Drive, Atlanta, GA 30332-0100, USA;* [b]*Department of Mechanical Engineering, Carnegie Mellon University, Pittsburgh, PA 15213, USA*

(*Received 6 March 2008; final version received 22 April 2008*)

Membrane-based separations are an attractive means to separate hydrogen from gas mixtures in order to use hydrogen in energy-related applications. Zeolite membranes are robust materials that are well suited to be used in harsh conditions, but they are not typically selective for hydrogen. Several studies have shown that highly selective separations of hydrogen are possible using zeolite membranes whose pore mouths have been chemically modified. An important challenge for materials of this kind is to develop methods by which hydrogen selectivity can be retained without significantly reducing the hydrogen flux possible with an unmodified zeolite membrane. Motivated by this, the effect of the pore mouth modification of silicalite was examined using atomic-scale simulations. We developed methods to mimic the chemical vapour deposition of Si and O atoms near the surface of a silicalite crystal, and examined the flux of CH_4 and H_2 through the resulting materials. Under some degrees of surface modification, the CH_4 flux was reduced much more than the H_2 flux. This observation indicates that careful control of surface modifying layers may be a useful means of tailoring the performance of zeolite membranes for H_2 separations.

Keywords: zeolites; membranes; molecular dynamics

1. Separation of hydrogen using pore-modified zeolites

Conventional fuel sources are rapidly being depleted. Hydrogen is one attractive new energy source since once it is produced it can be used with little negative environmental effect. The most practical methods for obtaining large quantities of H_2 use hydrocarbon sources from which H_2 can be produced by steam reforming or by partial oxidation with oxygen. A common characteristic of these methods is that other gases are also produced, so separating H_2 efficiently is important for both economic and environmental reasons [1]. Inorganic membranes have the potential to play an important role in these separations if membranes with suitable permselectivities and durability can be developed [2,3].

As a candidate for membrane-based separation of H_2, we will consider silicalite, the all-silica analog of ZSM-5 (structure code MFI, space group *Pnma*). This structure has a three-dimensional porous network with typical pore size of $\sim$5.5 Å [4]. Among all efforts to fabricate zeolite membranes, methods for making membranes from silicalite are the most fully developed [5–8].

A characteristic of silicalite that is common to essentially all zeolites is that its pores are too large to block the adsorption of small gas molecules mixed with H_2, so a separation cannot be achieved based on simple molecular sieving. Moreover, H_2 adsorption in silicalite is weaker than CO_2 or CH_4, two typical gases present during H_2 production. Experiments that have been performed with silicalite membranes using gas mixtures including H_2 have not yielded results with selectivities that would be desirable in H_2 separations [9–14]. The physical phenomena that make silicalite unselective for H_2 in these mixtures are also present for essentially all zeolites, so the limitations of this material cannot be solved simply by using another zeolite framework.

One avenue that may allow the properties of zeolite membranes to be improved for H_2 separations is to chemically modify the external surfaces of membranes. This strategy has been explored in two experimental studies using silicalite membranes [15,16] and one using surface modified hybrid membranes [17]. In these experiments, methyl diethoxy silane was attached to the surfaces of ZSM-5 membranes as a modifier with the aim of reducing the width of the pores at the membrane surface. Ideally, this modifying layer could enhance the selectivity of the membrane for H_2 by reducing the effective pore size for molecules entering the membrane but still allow rapid transport of adsorbed molecules through the membrane. In the experiments by Hong et al., the selectivity of the membrane increased from 1.6 to 33 for the H_2/CH_4. Unfortunately, this improvement in selectivity was coupled with a large reduction in net H_2 flux [15]. An interesting question generated from these

*Corresponding author. Email: david.sholl@chbe.gatech.edu

ISSN 0892-7022 print/ISSN 1029-0435 online

DOI: 10.1080/08927020802162900
http://www.informaworld.com

experiments is whether there is a regime where surface modifications of zeolite membranes can be made to improve the selectivity of the membrane for a small species such as H_2 without a large decrease in the H_2 flux.

In this study, we examined the effect of pore modification on H_2 and CH_4 transport through silicalite via molecular simulations. To model modified membranes, a modifying layer was constructed near the surface by adding individual Si and O atoms to an initially crystalline sample. The net flux of H_2 and CH_4 was then calculated for the modified silicalite membrane as well as an unmodified crystal. While molecular dynamics (MD) techniques have been developed to simulate transport through the zeolite membranes, most of them are based on the assumption that intracrystalline diffusion determines the transport rate [18–20]. To describe pore mouth modified zeolite membranes, however, the increased surface resistance associated with the modifying layer is a key factor. It is therefore vital that we use a calculation method that accounts for the impact of surface resistances during the operation of the membrane. To do this, we applied the local equilibrium flux method (LEFM) [21,22], a method that can calculate surface resistances rapidly from an atomically-detailed model of a membrane material by describing the local fluxes that exist at the gas-membrane interface.

2. Atomically-detailed model of pore mouth modification

To describe gas permeation through a modified zeolite membrane using molecular simulations, the atomic-scale configuration of the modified zeolite structure must be defined. In this section, we describe how a thin layer that mimics amorphous silica was added to the external surfaces of crystalline silicalite. The intention of this procedure was not to precisely model a specific experimental procedure, since detailed structural information about the modifying layers from the limited number of experimental studies that have been performed is not available.

The diffusion of molecules through silicalite crystals is anisotropic because of the anisotropy of silicalite's pores. Sinusoidal channels go along the crystallographic *x*-orientation, straight channels go along the *y*-orientation and although no pores exist along the *z*-orientation, net diffusion in the *z*-orientation can occur via diffusion in the *x* and *y*-orientation [23,24]. Since the *y*-orientation of silicalite provides the fastest intracrystalline diffusion for unmodified membranes [25], modifying layers were created on the surface of 2×2 unit cells in *xz* plane.

For simplicity in making modified zeolite structures, we modified surface structures by directly adding individual Si and O atoms. First, physically plausible positions are found via geometric criteria. Atoms were inserted only in positions where bond lengths, bond angles and coordination numbers are within physically available ranges. The criteria for each of these quantities was adapted from extensive simulations of amorphous silica zeolites by Mukhopadhyay et al. [26,27] and simulations of internal grain boundaries in silicalite by Newsome and Sholl [28].

To find positions where the criteria are satisfied, an atom is inserted at a random position near the surface. The inserted atoms are randomly chosen from Si and O with a Si:O ratio of 1:2. Each time an atom is inserted, a list of neighbour atoms is made to calculate bond lengths, bond angles and coordination numbers, with the latter defined as the number of bonds present within a specified range of bond lengths [26]. If all the criteria shown in Table 1 are satisfied for the inserted atom, then this atom is accepted. For example, if an inserted O atom forms bonds with Si atoms with bond lengths between 1.42 and 1.82 Å, Si–O–Si bond angles between 90° and 180°, O–Si–O bond angles between 80° and 140°, has a coordination number between 1 and 3, and has all O–O distances >2.21 Å, then the insertion of this O atom is accepted. If one (or more) of those criteria is not satisfied, then the trial position is rejected and the inserted atom is moved to a nearby position by a random walk. If no acceptable position can be found within 50 steps of the random walk, the atom is removed and a new insertion is begun.

The coordination number criteria for insertion on surface of silicalite are slightly different from those used previously to describe internal grain boundaries [28]. In the latter case, the allowable coordination numbers for Si were 3 to 5. When modifying the zeolite's surface, we allowed Si atoms to be inserted with coordination numbers from 1 to 5, to allow both the creation of new atoms on the external surface and bulk-like atoms. The valid coordination numbers for O atoms were defined to be the same as earlier work on grain boundary [28]. Atoms were inserted to randomly chosen positions within ± 5 Å from the surface, which was defined as the position of the topmost atoms of the zeolite including any atoms in the modifying layer that have already been deposited.

Once an atom is inserted as described above, a quenching procedure was used to relax the atomic positions. In this procedure, the potential energy, U_{ij}, of Si and O atoms was defined using the van Beest–Kramer–van Santen (BKS) interatomic potential for silica [29–31]. This potential, with the additional Lennard-Jones 24-6

Table 1. Criteria for inserting atoms as defined in text [26,27].

Si–O bond length [Å]	1.62 ± 0.20
O–O length[Å]	>2.21
Si–Si length[Å]	>2.79
Si–O–Si bond angle [deg]	135 ± 45
O–Si–O bond angle [deg]	110 ± 30
Coordination number of O	1–3
Coordination number of Si	1–5

Table 2. Parameters for the BKS potential [29,30,32].

q_{Si}: 2.4 [e] q_O: −1.2 [e]	O–O	Si–O	Si–Si
A [eV]	1388.7730	18003.7572	–
B [Å^{-1}]	2.76	4.87318	–
C [eVÅ^6]	175	133.5381	–
ϵ [kJ/mol]	0.04613	1.0834	1276.8E3
σ [Å]	2.2	1.3	0.4

terms suggested by Guissani and Guillot [32] for amorphous silica, has the form

$$U_{ij} = \frac{q_i q_j}{r_{ij}} + A_{ij}\exp(-b_{ij}r_{ij}) - \frac{c_{ij}}{r_{ij}^6} + 4\varepsilon_{ij}\left[\left(\frac{\sigma_{ij}}{r_{ij}}\right)^{24} - \left(\frac{\sigma_{ij}}{r_{ij}}\right)^{6}\right]. \quad (1)$$

Here, the subscripts i and j refer to Si and O atoms, q is the charge of an atom, A, b, c are parameters and r is an interatomic distance. The first term contains the long range electrostatic interaction between the effective charges and second and third terms represent covalent bonding interaction and short range repulsion between oxygen atoms. Parameters have been derived to stabilise the tetrahedral structures of amorphous silica. The parameters for the BKS potential are shown in Table 2 [29,30,32]. The electrostatic interactions were handled using the Wolf method with an α value of 0.345 Å^{-1} [33]. The potential cutoff was 12 Å.

During our MD simulations using this potential, temperature was controlled using the Nosé–Hoover thermostat and the equations of motion were integrated with the Verlet leapfrog algorithm with 0.905 fs time step. A temperature quench was performed by removing kinetic energy at the rate of 7.3×10^{15}K/s from 200 K until the kinetic energy vanishes. The structure that results from this procedure defines a local minimum on the potential energy surface. For computational efficiency, only the inserted atom and its neighbours were relaxed. We typically inserted multiple atoms before MD was used to relax the positions of these atoms.

The procedure defined above leaves a small number of highly undercoordinated atoms near the upper boundary of the modifying layer. The final stage of defining a modified layer was to examine the atomic density d in the layer in slices 1 Å thick normal to the zeolite's initial surface. The atom density in these slices abruptly drops from a roughly constant value inside the layer to zero outside the layer. In the region where this density drop occurs, we removed any Si atoms with coordination numbers of 1 or 2.

Figure 1 shows side views of modified silicalite with different degrees of modification. Although insertion attempts were made for positions within ±5 Å of the zeolite's surface, the great majority of inserted atoms lie on top of the surface rather than inside the zeolite pores. Figure 2 shows top views of unmodified and modified silicalite. After modification, the size of pores was reduced. It is reasonable to expect that this may reduce the flux of molecules into the pores when the crystal is used as a membrane.

One way to characterise the modifying layers in our simulated structures is to calculate the free volume in the layers available for diffusion of adsorbed molecules. Free volumes were measured by inserting spherical probes into the region of interest. To measure the available free volume accessible by CH_4 (H_2), a spherical probe of radius 1.9 Å (1.445 Å) was used. The radius of Si and O atoms were assigned as the van der Waals radii of $r_{Si} = 2.10$ Å and $r_O = 1.52$ Å. The position for a probe sphere was considered as the part of the free volume if no overlaps existed between the probe sphere and the Si and O atoms, and the free volume was defined by the fraction of feasible locations for probe spheres after $> 10^8$ trial insertions.

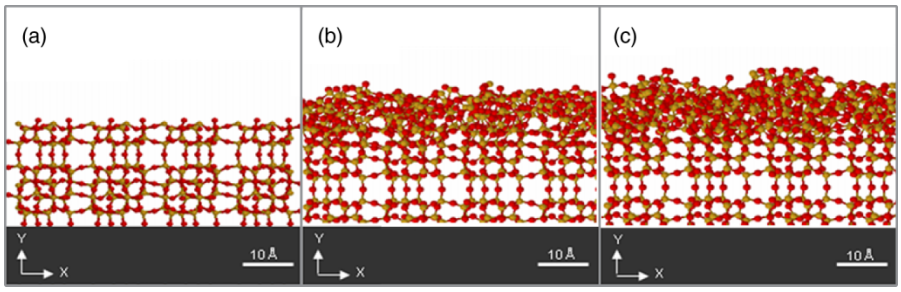

Figure 1. Side views of (a) unmodified silicalite and (b)–(c) surface modified silicalite with various degree of modification. As modification proceeds, the thickness of the modifying layer increases.

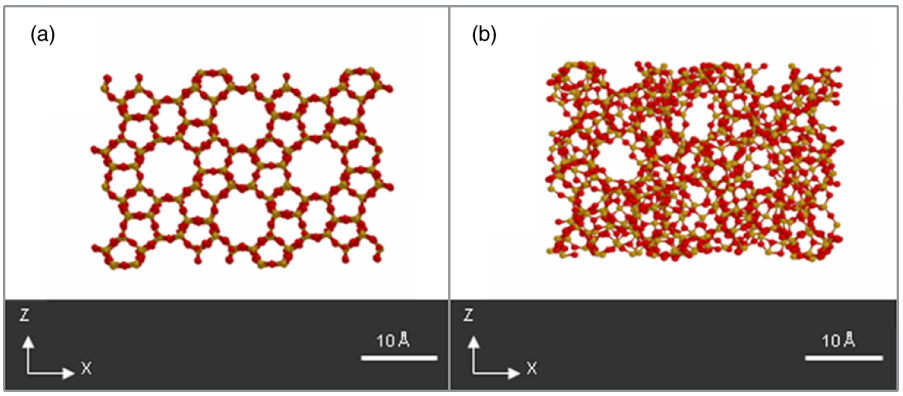

Figure 2. Top views of (a) unmodified silicalite and (b) surface modified silicalite.

We calculated the ratio of free volume per total volume in a region 2 Å thick in the *y*-direction located 1.5 ~ 3.5 Å above the initial surface of the crystalline silicalite. Figure 3 shows the free volume of six modified silicalite membranes as a function of the two-dimensional density of atoms in the modifying layers, *d*. Each membrane is numbered as 1 to 6. Since the probe sphere used for H_2 is smaller than for CH_4, the free volume is higher for H_2 in all cases. The free volume for each probe decreases steadily as more material is added to the modifying layer. For the membrane with the most Si and O atoms in the modifying layer, membrane 6, the free volume ratio for the CH_4 probe is reduced to 0.008, which is big reduction when comparing to 0.086 in crystalline silicalite. In addition, the difference in free volume between crystalline silicalite and the modifying layer for this membrane for the H_2 probe is less severe; these values reduced from 0.19 to 0.035, which differ by a factor of 5.

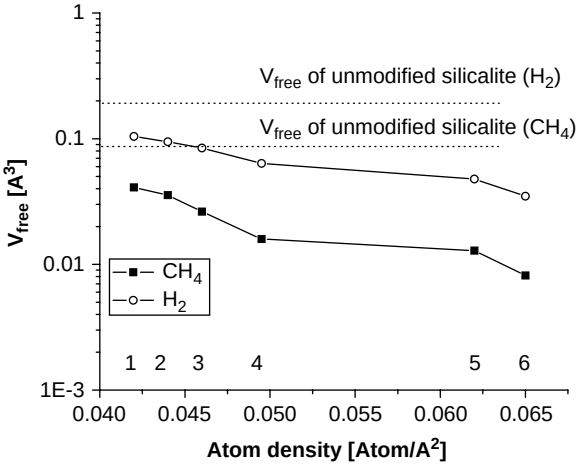

Figure 3. Free volume calculated in a 2 Å slice in the modifying layer on the modified silicalite membranes used in our calculations, shown as a function of the two-dimensional density of atoms in the modifying layers, *d*. Dashed lines indicate the free volume of unmodified silicalite.

3. Gas permeation through surface-modified membranes

3.1 The local equilibrium flux method

Molecules pass through a zeolite membrane in three steps. Molecules must adsorb to the crystal's external surface, then they diffuse through the crystal's pores and finally molecules desorb from the downstream surface of the zeolite. In most models for molecular transport through zeolite, surface effects are assumed to be far smaller than intracrystalline resistances. In this case, the steady-state flux of a single species permeating through a membrane can be calculated from [18,25,34]

$$J_{\text{ideal}} = \frac{1}{L}\int_{c_{\text{permeate}}}^{c_{\text{feed}}} D_{\text{t}}(c')\mathrm{d}c'. \qquad (2)$$

Here, c_{feed} (c_{permeate}) is the adsorbed concentration at the feed (permeate) side of the membrane, L is the membrane thickness and D_{t} is the transport diffusion coefficient of the adsorbed species. This diffusion coefficient, which is dependent on the concentration of the adsorbing species, can be calculated using equilibrium molecular dynamics (EMD) [25,34,35]. In the absence of surface resistances, the concentration of the adsorbates is defined by the equilibrium adsorption isotherm via the gas phase pressure on the feed and permeate side, P_{feed} and P_{perm}, respectively.

In the case of surface modified zeolites, surface resistances are key factors in the performance of the material. One widely used simulation technique to measure flux in the presence of surface resistances is dual control volume grand canonical molecular dynamics (DCV GCMD). This is a conceptually simple method in which the net flux, J, of molecules passing through a membrane is directly computed under nonequilibrium conditions. Unfortunately, this method is very computationally intensive and can only be applied to crystals much smaller than those relevant to current experiments [21,28,36]. The local equilibrium flux method (LEFM) offers a way to estimate surface resistances without

directly observing J [21]. The LEFM has been compared to DCV GCMD simulations of gas permeation through unmodified silicalite membranes by Newsome and Sholl [21,22]. Although the LEFM is not exact, it was shown to accurately estimate the size of surface resistances in a way that can be used to examine much wider ranges of operating conditions than is possible using DCV GCMD. Importantly for our purposes, the surface resistances associated with unmodified *y*-oriented silicalite membranes were shown to be small for all conditions we examine below. The LEFM has also been applied to estimate the role of surface resistances in carbon nanotube membranes [37]. In carbon nanotube membranes, surface resistances may be more important than for unmodified zeolites because of the extremely low resistance to mass transport that exists inside the membrane's pores [38–40].

The aim of the LEFM is to characterise the net membrane flux in terms of the local fluxes that exist under equilibrium conditions. If j_+ (j_-) is the one way flux from left to right (right to left) at any plane through the membrane, the net flux J is $J = j_+ - j_-$. If the system is at equilibrium, then $j_{eq} = j_+ = j_-$ and $J = 0$. The equilibrium flux, j_{eq} can be measured by counting molecules crossing an interface using equilibrium MD simulations. The LEFM assumes the net steady state flux can be estimated by the difference of the one way equilibrium fluxes at different effective pressures [21]. The total feed side flux is

$$J_{feed} \cong j_{eq}(P_{feed}) - j_{eq}(P_{ads}). \quad (3)$$

Here, P_{feed} is the actual gas phase pressure outside the membrane, while P_{ads} is an effective pressure in the membrane boundary layer. By writing $P_{ads} = P_{feed} - \delta P$, we can rewrite Equation (3) as

$$J_{feed} \cong j_{eq}(P_{feed}) - j_{eq}(P_{feed} - \delta P) = \delta P\left(\frac{dj_{eq}}{dP}|_{P_{feed}}\right). \quad (4)$$

Therefore, we can calculate the net flux on the feed side if we measure the local equilibrium flux at various pressures. In the case of interest to us where the surface resistance from a modifying layer appears only on the feed side, the intracrystalline flux can be calculated from

$$J_{intra} = \frac{1}{L}\int_{c_{permeate}}^{c_{ads}} D_t(c')\mathrm{d}c'. \quad (5)$$

In this case, c_{ads} is the adsorbate concentration that corresponds to the effective pressure P_{ads}. At steady state, the feed flux and intracrystalline flux obtained from Equations (4) and (5) must be the same. The net flux can be calculated by adjusting P_{ads} iteratively.

It is often convenient to describe net mass transfer through a membrane in terms of resistances associated with the different processes involved. Using this approach, the resistances to transport due to the feed side, intracrystalline region and permeate side can be defined as R_{ads}, R_{intra} and R_{des} [36]. If surface resistances on both the feed and the permeate side are negligible, then R_{ads} and R_{des} may be disregarded. The net flux associated with this idealised situation is related to R_{intra} by

$$J_{ideal} = \frac{\Delta c}{R_{intra}} \quad (6)$$

where Δc is the concentration change in adsorbed concentration from feed to permeate side and. The flux in this expression is the same as the flux defined in Equation (2). For the surface-modified membranes, we want to consider the situation where R_{des} is negligible but R_{ads} is not. The net flux through the membrane can then be expressed in terms of resistances to mass transport as

$$J = \frac{\Delta c}{R_{ads} + R_{intra}}. \quad (7)$$

In this expression, the flux is the net flux defined iteratively using Equations (4) and (5). From Equations (6) and (7), it is convenient to define the ratio of adsorption resistance to the intracrystalline resistance by

$$\frac{R_{ads}}{R_{intra}} = \frac{J_{ideal}}{J} - 1. \quad (8)$$

3.2 Equilibrium simulations of CH_4 and H_2 in surface-modified silicalite

In our calculations CH_4 and H_2 molecules were treated as rigid spherical molecules and only dispersive interactions were considered to describe the potential energy surface. A Lennard-Jones (LJ) pair-wise potential was used to calculate adsorbate–adsorbate interaction and adsorbate–zeolite interaction;

$$U_{ij} = 4\varepsilon_{ij}\left[\left(\frac{\sigma_{ij}}{r_{ij}}\right)^{12} - \left(\frac{\sigma_{ij}}{r_{ij}}\right)^{6}\right] \quad (9)$$

We used interaction parameters for CH_4 and H_2 from the literature [41]. These parameters are shown in Table 3. In many calculations for the adsorption in homogeneous zeolites, only the framework O atoms in the zeolite are considered to calculate the host-guest potential energy since Si atoms are shielded from the guest molecules

Table 3. Parameters for LJ potential [41].

	CH_4–O	H_2–O	CH_4–CH_4	H_2–H_2
ϵ [K]	133.3	51.233	147.9	34.02
σ [Å]	3.21	2.62	3.73	2.96

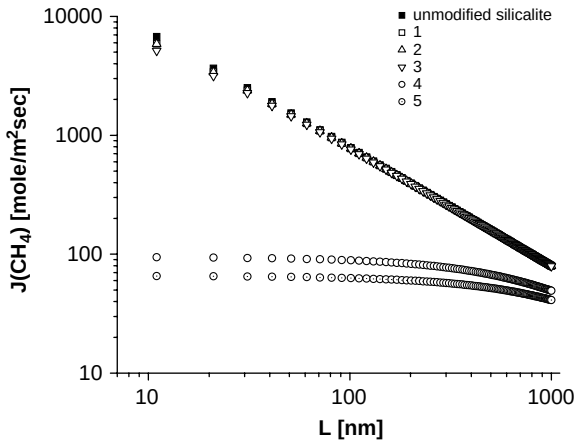

Figure 4. Net flux of CH_4 through surface modified silicalite. In every case, $P_{feed} = 10$ bar and $P_{perm} = 0.3$ bar.

[41,42]. In our calculations, however, we also considered the effect of the Si atoms on the total potential because Si atoms near the external surface can be exposed to the guest molecules. Interactions between Si atoms and guest molecules were described by a purely repulsive LJ-12 potential, that is, the first term of the Equation (9). The parameters for this potential were chosen as $\epsilon_{Si\text{-}Guest} = 200$ K, $\sigma = 1.5$ Å to create a repulsive force near the Si atoms but not to affect adsorption in a homogeneous silicalite.

Two assumptions were made in performing our calculations. First, the structure of the zeolite was assumed to be rigid. This assumption leads to a great reduction in the computational effort, since the potential energy surface defined by the zeolite can be pretabulated [41,42]. It is possible that local vibrations in the modifying layer could play a larger role in the transport of highly hindered molecules than in transport of the same molecules inside the zeolite pores. Inclusion of these vibrational degrees of freedom would be a useful topic to pursue in future extensions of this work. Second, the interactions of guest molecules with undercoordinated zeolite atoms on the surface of the membrane were treated with the same interaction potentials as fully coordinated zeolite atoms in the bulk material. In reality, it is likely that these undercoordinated atoms are terminated with hydroxyl or similar species [43,44]. By neglecting any differences in interaction potentials that might arise from these effects, our calculations are consistent with previous calculations for unmodified zeolite surfaces [21,36].

To calculate the intracrystalline flux of CH_4 and H_2 in Equation (5), we need the transport diffusivity, D_t and adsorption isotherms in bulk silicalite. For CH_4, we used previously calculated data [21,24]. The values for H_2 were calculated using EMD and grand canonical Monte Carlo (GCMC) simulation [21,24,45]. For all the simulations the cutoff distance for the interactions was set to 13 Å. For GCMC simulation to measure the adsorption isotherm, we used 2×10^7 Monte Carlo moves for equilibration, followed by 1×10^7 Monte Carlo moves for data collection. In our MD calculations, systems were initialised with 1.5×10^5 steps of canonical Monte Carlo moves and equilibrated by MD. Trajectories were measured for 10 ns with 1 fs time step with 30 trajectories.

The local equilibrium flux j_{eq} in Equation (4) was measured with various pressures using EMD with an Andersen thermostat [45]. The length of the gas region was 40 Å in the y-direction. Like previous MD simulations, the system was initialised by canonical Monte Carlo moves and equilibrated by MD [21]. Approximately 42 to 160 molecules were located in the total system and simulations were performed for 20 ns. From the forward and backward movement of molecules along the y direction, the local flux was calculated across various planes oriented perpendicular to the crystallographic y-orientation of the zeolite. The minimum local flux observed from this collection of planes was used for our LEFM calculations since this is the relevant flux for determining the net flux on the feed side. This minimum flux was observed to occur in the region of the modifying layer above the initial surface of crystalline silicalite that was characterised in terms of free volume in Figure 3.

3.3 Results

Using the methods described above, we examined the single-component flux of CH_4 and H_2 through silicalite membranes with various degrees of surface modification. We will discuss our results using the numbering system assigned to our simulated membranes in Figure 3. Figure 4 shows the net flux of CH_4 calculated with the LEFM as a function of membrane length, L, with $P_{feed} = 10$ bar and $P_{perm} = 0.3$ bar. It can be seen from Equation (7) that if the

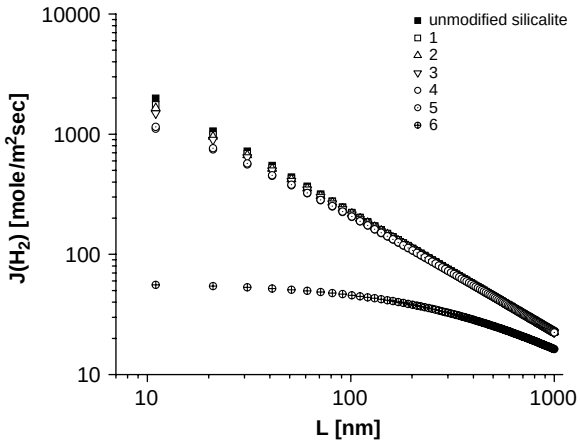

Figure 5. Net flux of H_2 through surface modified silicalite. In every case, $P_{feed} = 10$ bar and $P_{perm} = 0.3$ bar.

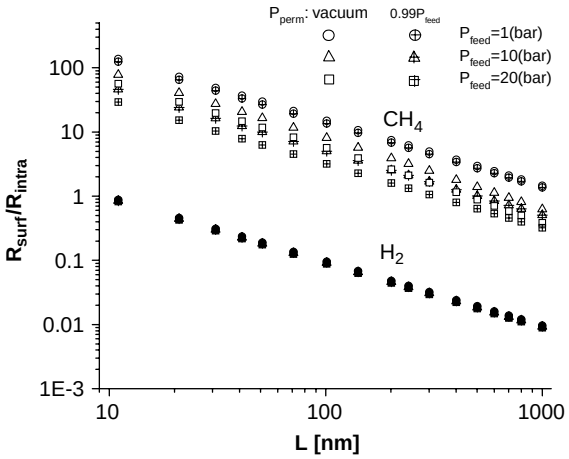

Figure 6. Surface resistance ratios as a function of membrane length, L, for surface-modified membrane 4. Results are shown for three values of P_{feed} and two values of P_{perm}. Open symbols represent CH_4 data, while closed symbols show H_2 data.

surface resistance is negligible, then a plot of log J versus log L is linear. This situation accurately describes the results in Figure 4 for membranes 1–3. This supports our earlier statement that the surface resistances of the unmodified membrane could be neglected in our description of the permeate side of the membrane. For larger degrees of modification, the curves in Figure 4 deviate strongly from linearity, indicating that the surface resistance becomes an important effect. These results are consistent with the free volume results shown in Figure 3. For membranes 4 and 5, the calculated fluxes are not very different and the free volume accessible to CH_4 in these two membranes is similar. For membrane 6, CH_4 could no longer permeate through the membrane, so the surface modification had blocked the pores to CH_4 molecules on MD time scales.

Figure 5 shows results similar to those in Figure 4 for the permeation of H_2 with $P_{feed} = 10$ bar and $P_{perm} = 0.3$ bar. For surface modifications for membranes 1–5, the H_2 flux is negligibly affected by the modifying layer. For membrane 6 the H_2 flux was significantly reduced by the modifying layer. For a membrane with $L = 1\,\mu m$ under these conditions, the H_2 flux was reduced by 72% compared to the unmodified silicalite membrane. Crucially, however, CH_4 was blocked by this modifying layer.

The ratios of adsorption resistance to intracrystalline resistances for CH_4 and H_2 are shown for a variety of operating conditions for membrane 4 in Figure 6. Figure 6 includes results with $P_{feed} = 1$, 10 and 20 bar. In this figure, circles are the results for membranes with a transmembrane pressure drop equal to the feed pressure, while crosses are for membranes where the pressure drop is only 1% of the feed pressure. For a given feed pressure, these two pressure drops span the full range of possible pressure drops. R_{ads}/R_{intra} is large when L is small because R_{intra} is proportional to L (see Equations (2) and (6)), while R_{ads} is only weakly dependent on L. The most important observation from Figure 6 is that for a broad range of operating conditions the surface resistance due to the modifying layer is much larger for CH_4 than for H_2. The magnitude of the surface resistance is more sensitive to the operating conditions for CH_4 than for H_2. While this is in part simply due to the much larger resistances that exist for CH_4, this sensitivity also stems from the fact that the range of pressures included in Figure 6 spans a larger range of adsorbate concentrations for CH_4 than for H_2 because of the stronger adsorption of CH_4.

Figure 7 summarises the ideal selectivity, that is, the ratio of single-component fluxes, of the membranes we have considered as the density of the modifying layer is increased. For membranes 1–3, the ideal selectivity is essentially that of the unmodified membrane, which significantly favours permeation of CH_4 under all operating conditions. As the thickness and density of the modifying layer increases, the ideal selectivity increases somewhat for membranes 4 and 5. In this range, the membrane is only selective for H_2 if the membrane thickness is less than 500 nm. Fabricating zeolite membranes with this thickness is currently a challenge [46,47]. For membrane 6, however, the ideal selectivity becomes infinity because CH_4 is excluded from the membrane. This modifying layer is selective for H_2 because of a simple molecular sieving mechanism. When both species can permeate through the membrane, the selectivity of the membrane when exposed to a mixed gas feed can differ from the ideal selectivity [48].

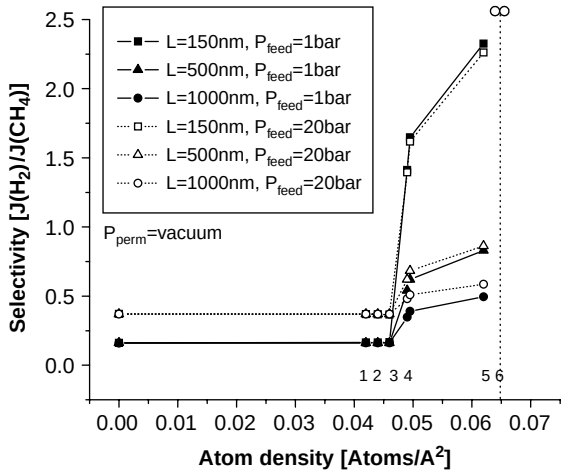

Figure 7. Ideal selectivity of H_2 relative to CH_4 as a function of the two-dimensional density of the modifying layers. Results are shown for two values of P_{feed} and three membrane thicknesses. In every case, P_{perm} was assumed to be a vacuum. Selectivity is infinity at membrane 6 since CH_4 is blocked.

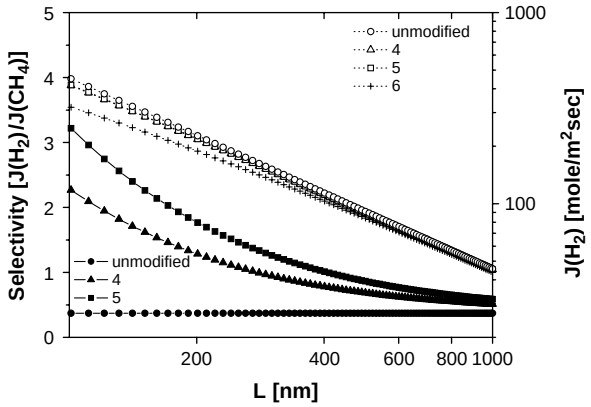

Figure 8. Ideal selectivity (filled symbols) and H_2 flux (open symbols) with an unmodified membrane and three modified membranes with various atom densities. Solid lines represent selectivity and dashed lines show flux.

This complication does not arise, however, if one species is excluded by molecular sieving.

Figure 8 shows the selectivity and H_2 flux for membranes 4–6 when $P_{\text{feed}} = 20$ bar and $P_{\text{perrm}} = 0$ bar. For the unmodified membrane, the ideal selectivity is smaller than 1 because CH_4 is more favoured by this membrane. For membrane 4 ideal selectivity decreases to 1 at $L = 270$ nm. The ideal selectivity of the membranes increased when degree of modification increased. For membrane 5, the ideal selectivity decreases to 1 at $L = 400$ nm. While the ideal selectivity of membranes 4 and 5 are larger than that of the unmodified membranes, we can observe that the H_2 flux with those membranes is decreased slightly from the flux of the unmodified membranes. For these two modified membranes, the reduction of CH_4 flux is far more significant than the H_2 flux. That is, the modified pore mouths can effectively block CH_4 only while they still allow transport of most H_2 molecules. The most useful membrane, however, would be one in which CH_4 was excluded from the membrane, such as membrane 6. With this membrane, the ideal selectivity is infinity. H_2 can still diffuse through this membrane with 72% of the flux through unmodified membrane when $L = 1000$ nm. It is likely that membranes with thicker modifying layer could also exclude H_2 molecules. To date, however, we have not performed simulation for membranes with modifying layers thicker than the one already obtained.

4. Discussion

Our results indicate that it is possible, at least in principle, to make modifications to zeolites such as silicalite to make membranes that can selectively transport H_2 from H_2/CH_4 mixtures without a catastrophic drop in the membrane's H_2 flux. These membranes take advantage of a situation where increased surface resistances for CH_4 transport make it possible to separate CH_4 from H_2 with high selectivity. The general concept of making a local modification in the surface structure of a zeolite membrane may be useful in other separations in addition to the H_2/CH_4 separation we have considered here. Although our simulations give some insight into the feasibility of this approach, several practical issues exist that would need to be carefully understood in order to use this idea experimentally. If the density of the modifying layer is too high, the porous layers could become completely blocked, stopping permeation of both H_2 and CH_4. It is not clear what level of control in the surface modification would be necessary to create layers that block CH_4 without blocking all molecular transport. Another complication in real zeolite membranes is that net transport through polycrystalline films involves contributions from both zeolitic and non-zeolitic pores. High quality zeolite membranes are assumed to be dominated by transport through zeolitic pores, but non-zeolitic pores are always present and are typically thought to reduce separation selectivity [49,50]. It is conceivable that efforts to modify zeolite surfaces could also block or reduce access to non-zeolitic pores, although our simulations provide no direct information on this possibility. The simulation methods we have introduced here may be of use in understanding what impact modifying layers could have on non-zeolitic pores in polycrystalline films.

Acknowledgement

Financial support from the National Science Foundation (CTS-0413027 and CTS-0556831) is gratefully acknowledged.

References

[1] US Department of Energy *Fuel Cell Handbook*, 7th edition, EG&G Technical Services, Inc. 2004.
[2] N.W. Ockwig and T.M. Nenoff, *Membranes for hydrogen separation*, Chem. Rev. 107 (2007), pp. 4078–4110.
[3] P. Kamakoti, B.D. Morreale, M.V. Ciocco, B.H. Howard, R.P. Killmeyer, A. Cugini, and D.S. Sholl, *Prediction of hydrogen flux through sulfur-tolerant binary alloy membranes*, Science 307 (2005), pp. 569–573.
[4] D.H. Olson, G.T. Kokotailo, S.L. Lawton, and W.M. Meier, *Crystal-structure and structure-related properties of ZSM-5*, J. Phys. Chem. 85 (1981), pp. 2238–2243.
[5] M. Yu, T.J. Amundsen, M. Hong, and J.L. Falconer, *Flexible nanostructure of MFI zeolite membranes*, J. Membr. Sci. 298 (2007), pp. 182–189.
[6] J. Motuzas, A. Julbe, and R.D. Noble, *Rapid synthesis of oriented silicalite-1 membranes by microwave-assisted hydrothermal treatment*, Microporous Mesoporous Mater. 92 (2006), pp. 259–269.
[7] A. Julbe, J. Motuzas, M. Arruebo, R.D. Noble, and J. Beresnevicius, *Synthesis and properties of MFI zeolite membranes prepared by microwave assisted secondary growth, from microwave derived seeds*, Stud. Surf. Sci. Catal. 158 (2005), pp. 129–136.
[8] J. Motuzas, A. Julbe, R.D. Noble, C. Guizard, Z.J. Beresnevicius, and D. Cot, *Rapid synthesis of silicalite-1 seeds by microwave assisted hydrothermal treatment*, Microporous Mesoporous Mater. 80 (2005), pp. 73–83.

[9] R. Lai and G.R. Gavalas, *ZSM-5 membrane synthesis with organic-free mixtures*, Microporous Mesoporous Mater. 38 (2000), pp. 239–245.
[10] M.C. Lovallo and M. Tsapatsis, *Preferentially oriented submicron silicalite membranes*, AIChE. J. 42 (1996), pp. 3020–3029.
[11] W. Dong and Y. Long, *Preparation and characterization of preferentially oriented continuous MFI-type zeolite membranes from porous glass*, Microporous Mesoporous Mater. 76 (2004), pp. 9–15.
[12] K. Aoki, K. Kusakabe, and S. Morooka, *Gas permeation properties of A-type zeolite membrane formed on porous substrate by hydrothermal synthesis*, J. Membr. Sci. 141 (1998), pp. 197–205.
[13] G.Q. Guan, T. Tanaka, K. Kusakabe, K.I. Sotowa, and S. Morooka, *Characterization of AIPO(4)-type molecular sieving membranes formed on a porous alpha-alumina tube*, J. Membr. Sci. 214 (2003), pp. 191–198.
[14] J.C. Poshusta, V.A. Tuan, E.A. Pape, R.D. Noble, and J.L. Falconer, *Synthesis and permeation properties of SAPO-34 tubular membranes*, Ind. Eng. Chem. Res. 37 (1998), pp. 3924–3929.
[15] M. Hong, J.L. Falconer, and R.D. Noble, *Modification of zeolite membranes for H_2 separation by catalytic cracking of methyldiethoxysilane*, Ind. Eng. Chem. Res. 44 (2005), pp. 4035–4041.
[16] T. Masuda, N. Fukumoto, M. Kitamura, and S.R. Mukai, *Modification of pore size of MFI-type zeolite by catalytic cracking of silane and application to preparation of H_2 separating zeolite membrane*, Microporous Mesoporous Mater. 48 (2001), pp. 239–245.
[17] S. Gopalakrishnan, Y. Yoshino, M. Nomura, B.N. Nair, and S. Nakao, *A hybrid processing method for high performance hydrogen-selective silica membranes*, J. Membr. Sci. 297 (2007), pp. 5–9.
[18] A.I. Skoulidas and D.S. Sholl, *Transport diffusivities of CH_4,He, Ne, Ar, Xe, and SF_6 in silicalite from atomistic simulations*, J. Phys. Chem. B. 106 (2002), pp. 5058–5067.
[19] D.S. Sholl, *Predicting single-component permeance through macroscopic zeolite membranes from atomistic simulations*, Ind. Eng. Chem. Res. 39 (2000), pp. 3737–3746.
[20] T.C. Bowen, J.L. Falconer, R.D. Noble, A.I. Skoulidas, and D.S. Sholl, *A comparison of atomistic simulations and experimental measurements of light gas permeation through zeolite membranes*, Ind. Eng. Chem. Res. 41 (2002), pp. 1641–1650.
[21] D.A. Newsome and D.S. Sholl, *Predictive assessment of surface resistances in zeolite membranes using atomically detailed models*, J. Phys. Chem. B 109 (2005), pp. 7237–7244.
[22] D.A. Newsome and D.S. Sholl, *Atomically detailed simulations of surface resistances to transport of CH_4, CF_4, and C_2H_6 through silicalite membranes*, Microporous Mesoporous Mater. 107 (2008), pp. 286–295.
[23] A.I. Skoulidas and D.S. Sholl, *Direct tests of the darken approximation for molecular diffusion in zeolites using equilibrium molecular dynamics*, J. Phys. Chem. B 105 (2001), pp. 3151–3154.
[24] A.I. Skoulidas and D.S. Sholl, *Molecular dynamics simulations of self-diffusivities, corrected diffusivities, and transport diffusivities of light gases in four silica zeolites to assess influences of pore shape and connectivity*, J. Phys. Chem. A 107 (2003), pp. 10132–10141.
[25] D.S. Sholl, *Understanding macroscopic diffusion of adsorbed molecules in crystalline nanoporous materials via atomistic simulations*, Acc. Chem. Res. 39 (2006), pp. 403–411.
[26] A.B. Mukhopadhyay, C. Oligschleger, and M. Dolg, *Molecular dynamics investigation of structural properties of a zeolite ZSM-5 based amorphous material*, Phys. Rev. B 67 (2003), p. 014106.
[27] A.B. Mukhopadhyay, C. Oligschleger, and M. Dolg, *Molecular dynamics investigation of relaxations in zeolite ZSM-5 based amorphous material*, J. Phys. Chem. B 108 (2004), pp. 16085–16092.
[28] D.A. Newsome and D.S. Sholl, *Molecular dynamics simulations of mass transfer resistance in grain boundaries of twinned zeolite membranes*, J. Phys. Chem. B 110 (2006), pp. 22681–22689.
[29] B.W.H. van Beest, GJ Kramer, and RA van Santen, *Force-fields for silicas and alumninophosphates based on ab initio calculations*, Phys. Rev. Lett. 64 (1990), pp. 1955–1958.
[30] G.J. Kramer, N.P. Farragher, B.W.H. van Beest, and R.A. van Santen, *Interatomic force-fields for silicas, aluminophosphates, and zeolites—derivation based on* ab initio *calculations*, Phys. Rev. B 43 (1991), pp. 5068–5080.
[31] A.J.H. McGaughey and M. Kaviany, *Thermal conductivity decomposition and analysis using molecular dynamics simulations—Part II Complex silica structures*, Int. J. Heat Mass Transfer 47 (2004), pp. 1799–1816.
[32] Y. Guissani and B. Guillot, *A numerical investigation of the liquid-vapor coexistence curve of silica*, J. Chem. Phys. 104 (1996), pp. 7633–7644.
[33] D. Wolf, P. Keblinski, S.R. Phillpot, and J. Eggebrecht, *Exact method for the simulation of coulombic systems by spherically truncated, pairwise r(-1) summation*, J. Chem. Phys. 110 (1999), pp. 8254–8282.
[34] E.J. Maginn, A.T. Bell, and D.N. Theodorou, *Transport diffusivity of methane in silicalite from equilibrium and nonequilibrium simulations*, J. Phys. Chem. 97 (1993), pp. 4173–4181.
[35] H. Mori, *Transport collective motion and brownian motion*, Prog. Theor. Phys. 33 (1965), pp. 423–428.
[36] M.G. Ahunbay, R.J. Elliott, and O. Talu, *Effect of surface resistances on the diffusion of binary mixtures in the silicalite single crystal membrane*, J. Phys. Chem. B. 109 (2005), pp. 923–929.
[37] D.A. Newsome and D.S. Sholl, *Influences of interfacial resistances on gas transport through carbon nanotube membranes*, Nano Lett. 6 (2006), pp. 2150–2153.
[38] H. Chen and D.S. Sholl, *Rapid diffusion of CH_4/H_2 binary mixtures in carbon nanotubes*, J. Am. Chem. Soc. 126 (2004), pp. 7778–7779.
[39] A.I. Skoulidas, D.M. Ackerman, J.K. Johnson, and D.S. Sholl, *Rapid transport of gases in carbon nanotubes*, Phys. Rev. Lett. 89 (2002), p. 185901.
[40] J.K. Holt, H.G. Park, Y.M. Wang, M. Stadermann, A.B. Artyukhin, C.P. Grigoropoulos, A. Noy, and O. Bakajin, *Fast mass transport through sub-2-nanometer carbon nanotubes*, Science 312 (2006), pp. 1034–1037.
[41] D. Dubbeldam, S. Calero, T.J.H. Vlugt, R. Krishna, T.L.M. Massen, and B. Smit, *Force field parametrization through fitting on inflection points in isotherms*, Phys. Rev. Lett. 93 (2004), p. 088302.
[42] M. Heuchel, R.Q. Snurr, and E. Buss, *Adsorption of CH_4–CF_4 mixtures in silicalite: simulation, experiment, and theory*, Langmuir 13 (1997), pp. 6795–6804.
[43] J.W. Han, J.N. James, and D.S. Sholl, *First principles calculations of methylamine and methanol adsorption on hydroxylated quartz (0001)*, Surf. Sci. 602 (2008), pp. 2478–2485.
[44] T.P.M. Goumans, A. Wander, W.A. Brown, and C.R.A. Catlow, *Structure and stability of the (001) alpha-quartz surface PCCP*, 9 (2007), pp. 2146–2152.
[45] D. Frenkel and B. Smit, *Understanding Molecular Simulation: From Algorithms to Applications*, Academic Press, London, 2002.
[46] Z. Wang, J. Hedlund, and J. Sterte, *Synthesis of thin silicalite-1 films on steel supports using a seeding method*, Microporous Mesoporous Mater. 52 (2002), pp. 191–197.
[47] J. Hedlund, J. Sterte, M. Anthonis, A.J. Bons, B. Carstensen, N. Corcoran, D. Cox, H. Deckman, W. De Gijst, P.P. de Moor, F. Lai, J. McHenry, W. Mortier, and J. Reinoso, *High-flux MFI membranes*, Microporous Mesoporous Mater. 52 (2002), pp. 179–189.
[48] S. Keskin and D.S. Sholl, *Screening metal-organic framework materials for membrane-based methane/carbon dioxide separations*, J. Phys. Chem. C. 111 (2007), p. 14055.
[49] J.C. Poshusta, R.D. Noble, and J. L. Falconer, *Temperature and pressure effects on CO_2 and CH_4 permeation through MFI zeolite membranes*, J. Membr. Sci. 160 (1999), pp. 115–125.
[50] T.C. Bowen, R.D. Noble, and J. L. Falconer, *Fundamentals and applications of pervaporation through zeolite membranes*, J. Membr. Sci. 245 (2004), pp. 1–33.